

# Probing the quantum-classical boundary with compression software

Hou Shun Poh<sup>1</sup>, Marcin Markiewicz<sup>2</sup>, Paweł Kurzyński<sup>1,3</sup>,  
Alessandro Cerè<sup>1</sup>, Dagomir Kaszlikowski<sup>1,4</sup>, and  
Christian Kurtsiefer<sup>1,4</sup>

<sup>1</sup>Center for Quantum Technologies, National University of Singapore, 3 Science Drive 2, Singapore 117543

<sup>2</sup>Institute of Physics, Jagiellonian University, ul. Stanisława Lojasiewicza 11, 30-348 Krakow, Poland

<sup>3</sup>Faculty of Physics, Adam Mickiewicz University, Umultowska 85, 61-614 Poznań, Poland

<sup>4</sup>Department of Physics, National University of Singapore, 2 Science Drive 3, Singapore 117542

**Abstract.** We adapt an algorithmic approach to the problem of local realism in a bipartite scenario. We assume that local outcomes are simulated by spatially separated universal Turing machines. The outcomes are calculated from inputs encoding information about a local measurement setting and a description of the bipartite system sent to both parties. In general, such a description can encode some additional information not available in quantum theory, i.e., local hidden variables. Using the Kolmogorov complexity of local outcomes we derive an inequality that must be obeyed by any local realistic theory. Since the Kolmogorov complexity is in general uncomputable, we show that this inequality can be expressed in terms of lossless compression of the data generated in such experiments and that quantum mechanics violates it. Finally, we confirm experimentally our findings using pairs of polarisation-entangled photons and readily available compression software. We argue that our approach relaxes the i.i.d. assumption, namely that individual bits in the outcome bit-strings do not have to be *independent and identically distributed*.

PACS numbers: 03.67.-a, 03.65.Ta, 42.50.Dv, 89.20.Ff

## 1. Introduction

In a standard Bell scenario [1] Alice and Bob share a bipartite system and each of them performs a randomly chosen local measurement on their subsystems. Then, they evaluate correlations between their outcomes. A violation of a suitable correlation-based Bell inequality refutes local realism.

The correlations are obtained by repeating the measurements on independent and identically distributed (i.i.d.) pairs and estimating the statistical frequencies  $p(x, y|a, b) = N(x, y|a, b)/N(a, b)$ , where  $N(x, y|a, b)$  is the number of times outcomes  $x$  and  $y$  are obtained for measurement settings  $a$  and  $b$ , and  $N(a, b)$  is the total number of measurements with settings  $a$  and  $b$ .

An interesting information theoretic approach to Bell inequalities was proposed in the 80's by Braunstein and Caves [2]. They constructed a test of local realism using the conditional Shannon entropy  $H(a|b) = H(a, b) - H(b)$ , where  $H(x) = -\sum_i p(x = x_i) \log_2 p(x = x_i)$ . This is a measure of how much information about Alice's outcomes is contained in Bob's outcomes. Although these inequalities are not tight, their immediate advantage is that they can be applied to experiments with more than two outcomes without any modifications. The simplest information-theoretic Bell inequality is

$$H(a_0|b_1) \leq H(a_0|b_0) + H(b_0|a_1) + H(a_1|b_0), \quad (1)$$

which holds for local realism, but it is violated by quantum physics.

Although the method of Braunstein and Caves offers a conceptually new approach, it requires the estimation of probabilities  $p(x, y|a, b)$  in an experiment. Therefore, actual implementations of such information-theoretic Bell tests are akin to the standard ones, and require a similar statistical analysis of the data strings obtained by Alice and Bob's measurement outcomes.

The Shannon entropy of a data string generated by an i.i.d. source has an important operational meaning: it tells us how much such a data string can be maximally compressed without losses [3]. However, Shannon's source coding theorem does not give a prescription for how to achieve this maximum compression.

For most data strings it is hard or impossible to prove that a compression algorithm is optimal. However, this does not stop us from introducing the concept of a *best possible* compression algorithm for a given data string  $x$ . This is exactly the idea behind the Kolmogorov complexity. More formally, the concept of Kolmogorov complexity requires a reference to a universal model of computation, for example a universal Turing machine (UTM). In this case the Kolmogorov complexity  $K(x)$  of a data string  $x$  is the length  $l(\Lambda)$  of the shortest program  $\Lambda$ , which, when fed into a UTM, produces an output string  $x$ . In general,  $K(x)$  is uncomputable. However, realistic compression algorithms can bound  $K(x)$  from above [4]. Formally, this means  $K(x) \leq C(x)$ , where  $C(x)$  is the length of the compressed string. A notable property of compression algorithms is that they can be applied to data strings that are generated by non-i.i.d. sources.

In this paper, we show that one can observe violations of local realism by studying the compression ratio of realistic compression algorithms, applied to outcomes of Bell

tests, and derive a compression-based Bell inequality. We then test this inequality in a real experiment measuring polarizations of pairs of entangled photons, and find a violation of the compression-based inequality for properly chosen local measurement settings, and a properly chosen compression algorithm. We note that our approach is related to an earlier one by Fuchs [5], and that an alternative approach to non-i.i.d. sources was discussed by Gill [6].

## 2. Algorithmic approach to Bell scenario

The core of any test for local realism is to acquire some information about possible hidden variables from measurement outcomes. The standard approach for Bell tests is based on the statistical inference of correlations between measurements. This implies repeating an experiment many times, sorting the results according to the measurement basis, and estimating the probability of each possible outcome from the observed frequencies. The algorithmic approach we present instead considers the output of a long sequence of measurements, the strings  $x$  and  $y$ , as primitives. The analysis of these strings, combined with the sequence of measurement bases, relies on their complexity, not on the statistics of the individual measurements outcomes.

This algorithmic model of a Bell test can be designed, in its most general form, in terms of input programs, UTMs, and their corresponding outputs. We can describe the sequence of measurement results of each party, independently, as the output of a UTM to which, in addition to the sequence of basis settings, the program  $\Lambda$  has been supplied, as shown in the top part of figure 1. We are interested in detecting any correlation between two parties, so we introduce two spatially separated UTMs:  $UTM_A$  and  $UTM_B$ , with the corresponding outputs,  $x$  and  $y$ . We assume that the two machines are supplied with a common input program  $\Lambda$  that can encode the physical description of the test system, and additional programs for each UTM encoding the sequence of local measurement settings  $a_j$  and  $b_k$  ( $j, k = 0, 1$ ). The spatial separation of the two parties ensures that  $a_j$  and  $b_k$  are only accessible to their corresponding UTM. This situation is depicted in the lower part of figure 1.

The Church-Turing thesis, in the Deutsch formulation, states that *a universal computing device can simulate every physical process* [7]. If there is a local hidden variable theory that describes the outputs of the test system above, it can be encoded in the program  $\Lambda$ . An experimental result that cannot be simulated by a our UTMs would therefore falsify any local realistic description of that process.

### 2.1. Analysis of the outcome strings

Similarly to a standard Bell test, we sort the bits of  $x$  and  $y$  into four pairs of strings, based on the corresponding measurement basis:  $\{x_0, y_0\}$ ,  $\{x_0, y_1\}$ ,  $\{x_1, y_0\}$  and  $\{x_1, y_1\}$ . To quantify how much information is shared between the strings of each pair we use the *Normalized Information Distance* (NID) introduced in [8]. This distance, based on the

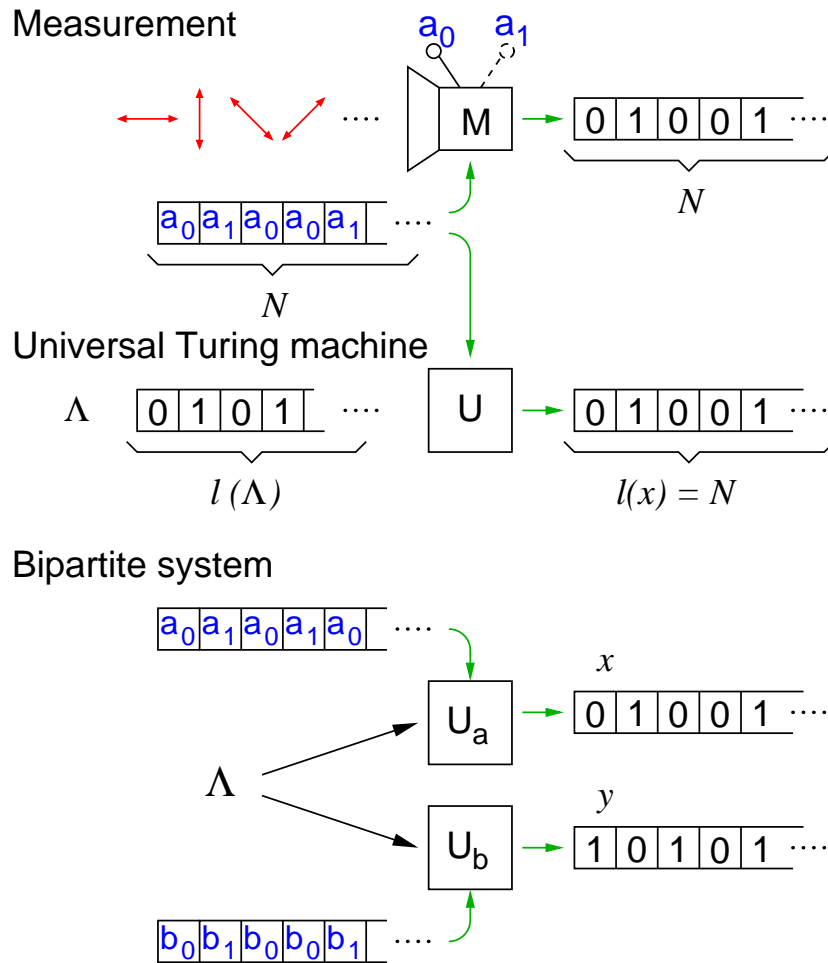


**Figure 1.** Measurement:  $N$  particles enter a measuring device characterized by two polarizer settings  $a_0$  and  $a_1$  generating  $N$ -outcome bit strings. A Universal Turing machine (UTM) fed with a program  $\Lambda_i$  and information about the settings  $a_0$  and  $a_1$  can reproduce the string of length  $N$ . The bottom part shows a model to reproduce correlated strings  $x$  and  $y$  generated from measurements on a bipartite system with local UTMs and a common program  $\Lambda$ .

Kolmogorov complexity, compares two strings  $x$  and  $y$  without any knowledge about their origin, and is a metric up to a correction  $(\log_2 N)/N$ , where  $N$  is the length of strings  $x$  and  $y$ . The NID is defined as

$$\text{NID}(x, y) = \frac{K(x, y) - \min\{K(x), K(y)\}}{\max\{K(x), K(y)\}}, \quad (2)$$

where  $K(x, y)$  is the Kolmogorov complexity of the string obtained by concatenating  $x$  and  $y$ . In general,  $K(x, y) \leq K(x) + K(y)$ , and  $0 \leq \text{NID}(x, y) \leq 1$ . If both strings are the same (i.e.,  $x = y$ ),  $K(x, y) = K(x) = K(y)$  and consequently  $\text{NID}(x, y) = 0$ . On the other hand, if  $x$  and  $y$  are completely independent,  $K(x, y) = K(x) + K(y)$ , so  $\text{NID}(x, y) = 1$ .

## 2.2. Algorithmic Bell inequality

We now use the metric properties of NID to construct a Bell inequality, similar to the approach used before in [9, 10, 11, 12]. The NID obeys the triangle inequality

$$\text{NID}(x, y) + \text{NID}(y, z) \geq \text{NID}(x, z), \quad (3)$$

where we use the the result strings for different settings on each side:

$$\text{NID}(x_0, y_0) + \text{NID}(y_0, y_1) \geq \text{NID}(x_0, y_1). \quad (4)$$

However,  $\text{NID}(y_0, y_1)$  cannot be determined experimentally because the strings  $y_0$  and  $y_1$  cannot be obtained at the same time since they come from incompatible measurements. Thus, we follow a standard reasoning used in the derivations of all known Bell inequalities, referred to as *counterfactual definiteness*, which states that it is admissible to consider outcomes of unperformed experiments. We apply it to our case, assuming that it is possible to associate a definite Kolmogorov complexity to a string that has not been generated. Using a second triangle inequality  $\text{NID}(x_1, y_0) + \text{NID}(x_1, y_1) \geq \text{NID}(y_0, y_1)$ , and combining it with (4), we get

$$\text{NID}(x_0, y_0) + \text{NID}(x_1, y_0) + \text{NID}(x_1, y_1) \geq \text{NID}(x_0, y_1). \quad (5)$$

As mentioned above, the NID is only approximately a metric, therefore the above inequality holds only up to a term  $(\log_2 N)/N$ . For convenience, we further introduce a parameter  $S'$  that quantifies the violation of inequality (5):

$$S' = \text{NID}(x_0, y_1) - \text{NID}(x_0, y_0) - \text{NID}(x_1, y_0) - \text{NID}(x_1, y_1) \leq 0. \quad (6)$$

A violation of the local realism hypothesis occurs if  $S'$  is positive.

Before moving on to testing the positivity of  $S'$ , we have to address a problem that also appears in standard Bell scenarios: every time the experiment is carried out (with all  $N$  particles and settings) with the same preparation, the resulting local strings  $x_j$  and  $y_k$  will be different. We therefore assume *uniform complexity*: for every two repetitions of the experiment  $i$  and  $i'$ , the complexity of the generated strings remains the same:  $K_i(x_j) = K_{i'}(x_j)$  and  $K_i(x_j, y_k) = K_{i'}(x_j, y_k)$ , up to a term  $(\log_2 N)/N$ . It follows that if inequality (6) is violated, either local realism or uniform complexity are invalid. This is especially relevant for experimental verifications where the bases  $\{a_j, b_k\}$  for each particle are not chosen randomly. It is worth noting that i.i.d. implies uniform complexity, as can be seen by segmenting a long string from a stream of i.i.d. particles. Therefore, the class of models rejected by inequality (6) is at least as large as the one rejected by standard Bell tests. We expect that it is possible to find non-i.i.d. systems with uniform complexity and, consequently, a violation of inequality (6) would reject a larger class of models.

## 3. Estimation of the Kolmogorov complexity of a string

In general, the Kolmogorov complexity of a string cannot be evaluated, but it can be estimated. One can adopt two conceptually different approaches. The first one, based

on statistics, results in an inequality similar to (1). We will briefly discuss it, however our main focus is the algorithmic approach.

### 3.1. Statistical estimation

For an ensemble  $X$  of strings, and assuming i.i.d., the expected Kolmogorov complexity for each string is equal to the Shannon entropy  $H(X)$  [13]. In experiments, the value of  $H(X)$  can be inferred by repeated measurements, and a statistical derivation of the probability distribution leading to  $H$  from the frequency of measurements outcomes. Replacing the Kolmogorov complexity with Shannon entropy, we obtain a measurable expression for NID:

$$\langle \text{NID}(x, y) \rangle = \frac{H(x, y) - \min\{H(x), H(y)\}}{\max\{H(x), H(y)\}}. \quad (7)$$

Assuming the probability distributions of standard quantum mechanics ( $QM$ ), it is straightforward to show that for maximally entangled polarization states of two photons and linear polarizers, inequality (5) becomes an entropic Bell inequality similar to (1). The conditional Shannon entropy only depends on the angle  $\theta$  between measurement directions  $a$  and  $b$  [2]:  $H^{QM}(x|y) = H^{QM}(y|x) \equiv H(\theta)$ . From Bayes's theorem,  $H(x, y) = H(x|y) + H(y) = H(y|x) + H(x)$ , hence  $H^{QM}(x) = H^{QM}(y)$ . By substitution, we obtain  $\langle \text{NID}(x, y) \rangle = H(\theta)$ . Braunstein and Caves showed that for coplanar measurements satisfying  $\vec{a}_0 \cdot \vec{b}_1 = \cos 3\theta$  and  $\vec{a}_0 \cdot \vec{b}_0 = \vec{a}_1 \cdot \vec{b}_0 = \vec{a}_1 \cdot \vec{b}_1 = \cos \theta$ , inequality (1) is violated for an appropriate range of  $\theta$ . We can directly calculate the expected value of  $S'$  as a function of  $\theta$  for the case of maximally polarization entangled photon pairs. We plot  $S'$  in figure 2(a) as a benchmark for the experimental values. Under this geometry, we find a maximal violation of  $S' = 0.24$  for  $\theta = 8.6^\circ$ .

### 3.2. Algorithmic estimation

It is possible to avoid a statistical estimation: the Kolmogorov complexity can be well approximated by compression algorithms [4]. For a string  $x$ , we define  $C(x)$  as the length of the string resulting from the compression of  $x$ .

Following [4], we introduce the *Normalized Compression Distance* (NCD):

$$\text{NCD}(x, y) = \frac{C(x, y) - \min\{C(x), C(y)\}}{\max\{C(x), C(y)\}}. \quad (8)$$

Replacing NID with NCD in inequality (6) leads to a new inequality:

$$\begin{aligned} S' \rightarrow S = & \text{NCD}(x_{a_0}, y_{b_1}) - \text{NCD}(x_{a_0}, y_{b_0}) \\ & - \text{NCD}(x_{a_1}, y_{b_0}) - \text{NCD}(x_{a_1}, y_{b_1}) \leq 0. \end{aligned} \quad (9)$$

This expression can be tested in a real experiment because the NCD is operationally defined. Moreover, it was shown in [4] that NCD is also a metric up to a term  $(\log_2 N)/N$ , therefore inequality (9) holds up to the same term.

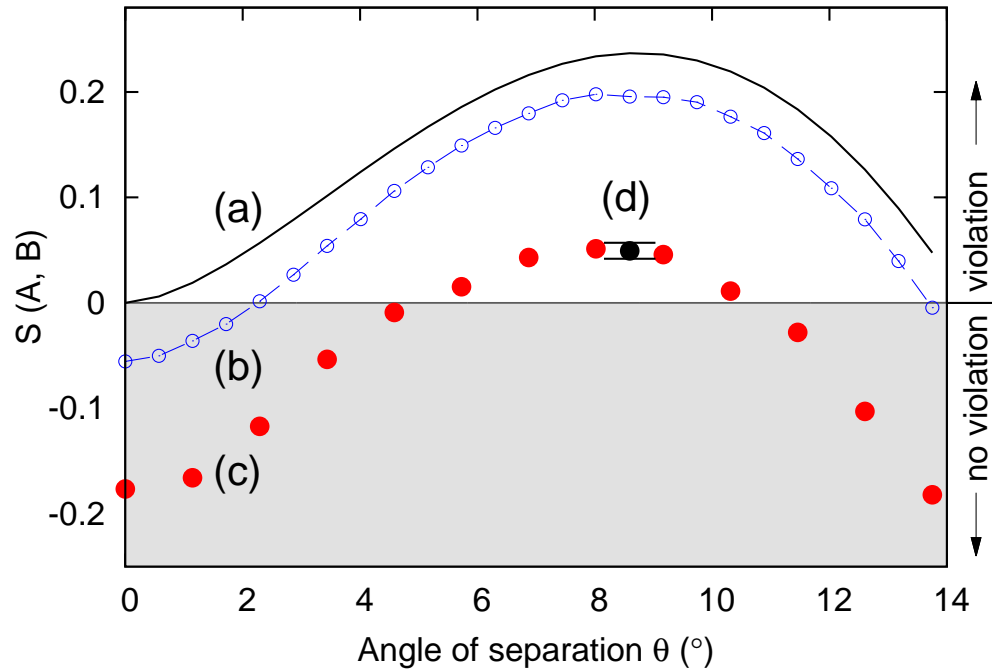


**Figure 2.** Plots of  $S$  versus angle of separation  $\theta$ . (a) Result obtained from Eq. (7), (b) result obtained from using the LZMA compressor on numerically generated data, (c) measurement of  $S$  in the experiment shown in figure 5, and (d) longer measurement at the optimal angle  $\theta = 8.6^\circ$ .

#### 4. Choice of compressor

Most compression algorithms use some prediction about the data composition. If it matches this prediction, the compression can be done efficiently. To conduct an experiment we need to ensure the suitability of the compression software we use to evaluate the NCD. For this, we numerically simulate the outcome of an experiment based on a distribution of results predicted by quantum physics.

In order to evaluate the NCDs of the binary strings, we need to choose a compression algorithm that performs close to the Shannon limit [3]. This is necessary to ensure that the NCD is a good approximation of the NID, and that it does not introduce any unintended artifacts that lead to an overestimation of the violation. Preferably we want to work in the regime where the obtained NCDs always underestimate the violation. For this purpose, we characterized four compression algorithms implemented by freely available compression programs: LZMA [14], BZIP2 [15], GZIP [16] and LZW [17]. To eliminate the overhead associated with the compression of ASCII text files, we save data in binary format.

For this characterization, and the following simulation of the experiment, we need to generate a “random” string of bits (1, 0) or pairs of bits (00, 01, 10, and 11) of various length with various probability distributions. We generate these strings using the *MATLAB* [18] function *randsample()* that uses the pseudo random number generator

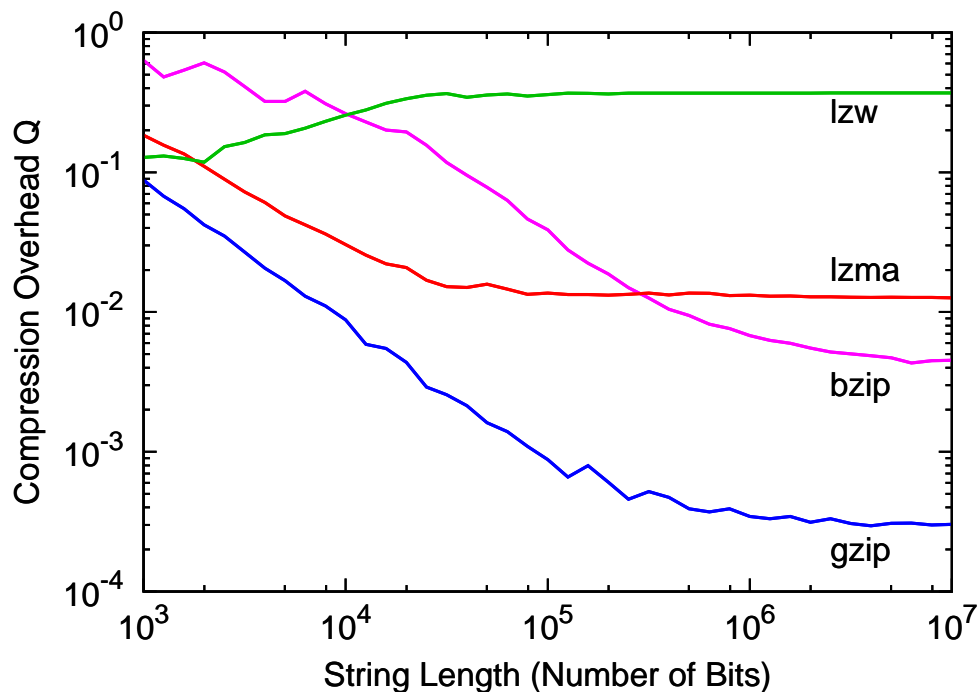


**Figure 3.** Comparison of the compression overhead  $Q$  obtained using four different compression algorithms on pseudo-random strings of varying lengths. The expected value for an ideal compressor is 0. From this characterization we can exclude LZW as a useful compressor for our application.

*mt19937ar* with a long period of  $2^{19937} - 1$ . It is based on the Mersenne Twister [19], with ziggurat [20] as the algorithm that generates the required probability distribution. The complexity of this (deterministic) source of pseudorandom numbers should be high enough to *not* be captured as algorithmic.

The first part of this characterization involves establishing the minimum string length required for the compression algorithms to perform consistently. We start by generating binary strings,  $x$ , with equal probability of 1's and 0's, i.e. random strings, of varying length. For each  $x$ , we evaluate the compression overhead  $Q$  as

$$Q = \frac{C(x) - H(x)}{l(x)}. \quad (10)$$

For a good compressor, we expect  $Q$  to be close to 0. From figure 3, it can be seen that for all the compressors,  $Q$  starts to converge after about  $10^5$  bits, setting the minimum string length required for the compressors to work consistently.

In the second part of this characterization, test the compressors with strings with a known amount of correlation. We generate a random string  $x$  of length  $10^7$  using the same technique already described. We then generate a second string  $y$  of equal length and with probability  $p$  of being correlated to  $x$ . For  $p = 0$  the two strings are equal, i.e. perfectly correlated. For  $p = 0.5$  they are uncorrelated. Strings  $x$  and  $y$  are combined to form the string  $xy$ . To avoid artifacts due to the limited data block size of the compression algorithms, the elements of  $x$  and  $y$  are interleaved: for example, for string



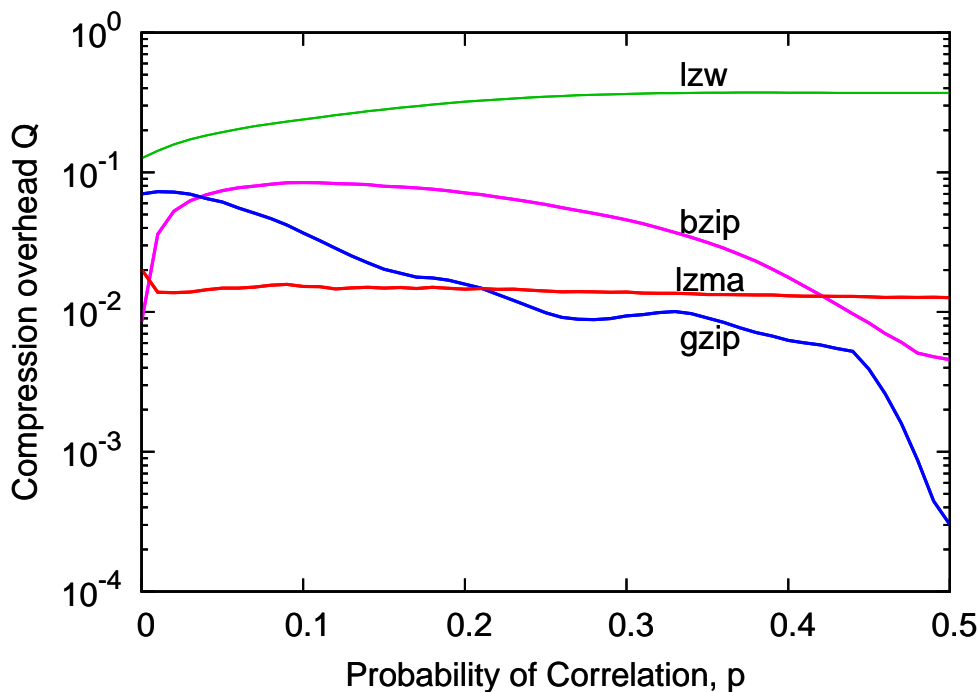


**Figure 4.** Compression overhead  $Q$  for the string  $xy$  as a function of the probability of pairwise correlation  $p$  between the bits of the generating strings  $x$  and  $y$  for three different compressors: BZIP2, GZIP, and LZMA.

$x = (0, 0, 0)$  and  $y = (1, 1, 1)$ , the resulting concatenated string is  $xy = (0, 1, 0, 1, 0, 1)$ . The same interleaving procedure is also implemented for the strings generated in the experiment, as described later on. We then compress  $xy$  and evaluate the compression overhead  $Q$  as a function of  $p$ . The results for different compressors are shown in figure 4. Although there are ranges of  $p$  where BZIP2 and GZIP perform better than LZMA, the latter shows a more uniform performance over the entire interval of  $p$ . On the other hand, LZW performs poorly in all respects. It is reasonable to assume that the use of LZMA should reduce the possibility of artifacts in the estimation of the NCD also for the data obtained from the experiment.

In general, our method can be used for data from any source by finding a suitable compression algorithm [4]. Thus, we are not limited to i.i.d. sources, as it is commonly assumed in standard statistical ensemble-based experiments, like, for instance, Bell-type tests.

The numerical simulation also verifies the angle that maximizes the violation of inequality (9). The results of this simulation are presented in figure 2.

## 5. Experiment

In our experiment (see figure 5), the output of a grating-stabilized laser diode (LD, central wavelength 405 nm) passes through a single mode optical fiber (SMF) for spatial mode filtering, and is focused to a beam waist of  $80 \mu\text{m}$  into a 2 mm thick BBO crystal

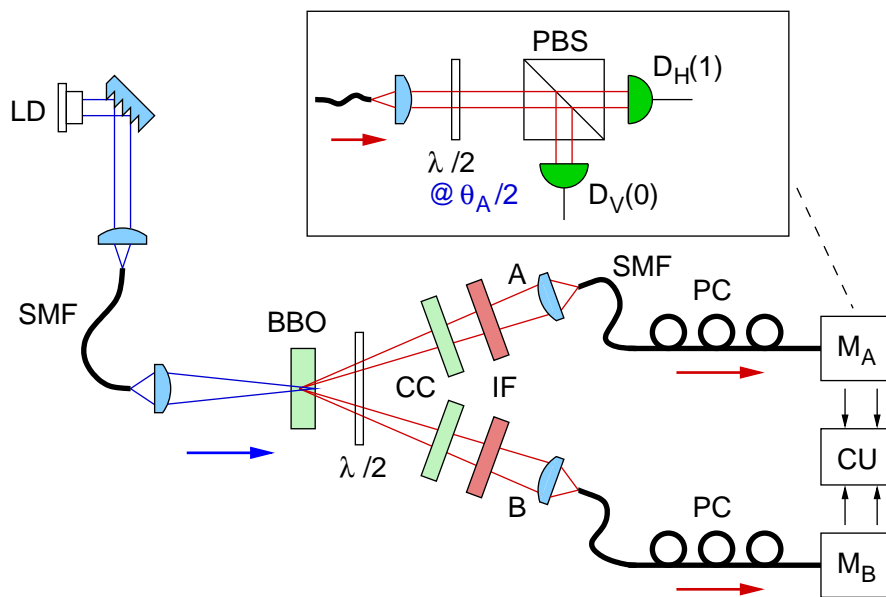


**Figure 5.** Schematic of the experimental set-up. Polarization correlations of entangled-photon pairs are measured by the polarization analyzers  $M_A$  and  $M_B$ , each consisting of a half wave plate ( $\lambda/2$ ) followed by a polarization beam splitter (PBS). All photons are detected by Avalanche photodetectors  $D_H$  and  $D_V$ , and registered in a coincidence unit (CU).

cut for type-II phase-matching. There, photon pairs are generated via spontaneous parametric down-conversion (SPDC) in a slightly non-collinear configuration. A half-wave plate ( $\lambda/2$ ) and a pair of compensation crystals (CC) take care of the temporal and transversal walk-off [21]. Two spatial modes ( $A$ ,  $B$ ) of down-converted light, defined by the SMFs for 810 nm, are matched to the pump mode to optimize the collection [22]. In type-II SPDC, each down-converted pair consists of an ordinary and extraordinarily polarized photon, corresponding to horizontal ( $H$ ) and vertical ( $V$ ) in our setup. A pair of polarization controllers (PC) ensures that the SMFs do not affect the polarization of the collected photons. To arrive at an approximate singlet Bell state, the phase  $\phi$  between the two decay possibilities in the polarization state  $|\psi\rangle = 1/\sqrt{2}(|H\rangle_A|V\rangle_B + e^{i\phi}|V\rangle_A|H\rangle_B)$  is adjusted to  $\phi = \pi$  by tilting the CC.

In the polarization analyzers (inset of figure 5), photons from SPDC are projected onto arbitrary linear polarization by  $\lambda/2$  plates, set to half of the analyzing angles  $\theta_{A(B)}$ , and polarization beam splitter (extinction ratio 1/2000 and 1/200 respectively for transmitted and reflected arm) in each analyzer. Photons are detected by avalanche photo diodes (APD), and corresponding detection events from the same pair identified by a coincidence unit if they arrive within  $\approx \pm 3$  ns of each other.

The quality of polarization entanglement is tested by probing the polarization correlations in a basis complementary to the intrinsic HV basis of the crystal. With interference filters (IF) of 5 nm bandwidth (FWHM) centered at 810 nm, in the  $45^\circ$  linear polarization basis we observe a visibility  $V_{45} = 99.9 \pm 0.1\%$ . The visibility in the natural

H/V basis of the type-II down-conversion process also reaches  $V_{HV} = 99.9 \pm 0.1\%$ . A separate test of a CHSH-type Bell inequality [23] leads to a value of  $S = 2.826 \pm 0.0015$ . This indicates a high quality of polarization entanglement; the uncertainties in the visibilities are obtained from propagated Poissonian counting statistics.

### 5.1. Measurement and Data Post-processing

In the realization of this proof of principle experiment, we did not intend to provide a loophole-free demonstration. Due to the limited efficiency of the APD detectors, we assume that the fraction of the photon we detected is a fair representation of the entire ensemble (fair sampling assumption). Similarly, even if Alice and Bob are not space-like separated, we assume that no communication happens between the two measurements. Moreover, the basis choice is not random, as expected in an ideal Bell-like experiment. We instead set the basis and record the number of events in a fixed time. We are assuming that the state generated by the source, and all the other parameters of the experiment, do not change between experimental runs.

The basic measurement lasts 60s, during which we record an average of  $16 \times 10^3$  two-fold coincidences between detectors at  $A$  and  $B$ . A detection event at the transmitted output of each PBS is associated with 0, reflected one with 1. Three- and four-fold coincidences, as well as two-fold coincidences between detectors belonging to the same party, correspond to multiple pairs of photons generated within the coincidence time window. The rate of these events is negligible, therefore we discarded them.

In order to avoid biases due to the asymmetries in detector efficiencies, to measure one basis  $(a_j, b_k)$  we also measure three complementary basis:  $(a_j + 45^\circ, b_k)$ ,  $(a_j, b_k + 45^\circ)$ , and  $(a_j + 45^\circ, b_k + 45^\circ)$ . A rotation by  $45^\circ$  effectively swaps the roles of the transmitted and reflected detectors. Each party, when measuring on the rotated basis, needs to apply a *NOT* operation to the measurement outcome. The results of these four measurements are combined into two binary files,  $x(a_j, b_k)$  and  $y(a_j, b_k)$ , by interleaving their respective bits. In order to obtain long enough strings for a stable compression, see figure 3, this measurement is repeated 11 times and the results concatenated, obtaining strings of average length  $10^5$  bits.

For each angle of separation  $\theta$ , we measure four bases  $(a_0, b_0)$ ,  $(a_1, b_0)$ ,  $(a_1, b_1)$ , and  $(a_0, b_1)$ , then calculate the NCD between  $x(a_j, b_k)$  and  $y(a_j, b_k)$  using Eq. (8), in order to obtain the value of  $S$ .

## 6. Results

The inequality is experimentally tested by evaluating  $S$  in Eq. (9) for a range of  $\theta$ ; the results [points (c), (d) in figure 2] are consistently lower than the trace (a) calculated via entropy using Eq. (7), and than a simulation with the same compressor (b). This is because the LZMA Utility is not working exactly at the Shannon limit, and also due to imperfect state generation and detection.

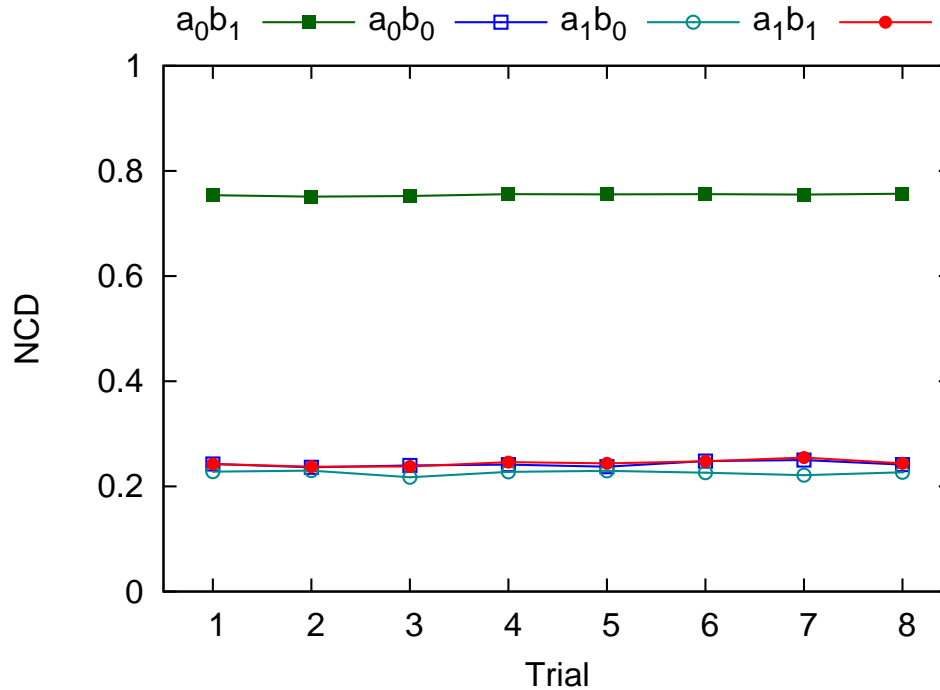


**Figure 6.** Measured value of the NCD for 8 trials for the four bases  $(a_0, b_0)$ ,  $(a_1, b_0)$ ,  $(a_1, b_1)$ , and  $(a_0, b_1)$ , and fixed angle  $\theta = 8.6^\circ$ . The evident stability of the values supports the uniform complexity assumption.

Although we set out in this work to avoid a statistical argument in the interpretation of measurement results, we do resort to statistical techniques to assess the confidence in an experimental finding of a violation of inequality (9). To estimate an uncertainty of the experimentally obtained values for  $S$ , we set  $\theta = 8.6^\circ$ , for which we expect the maximum violation, and collected results from a larger number of photon pairs. We then repeated the measurement of  $S$ , as described in the previous section, 8 times, and considered the average value and standard deviation of this set obtaining the final result of  $S(\theta = 8.6^\circ) = 0.0494 \pm 0.0076$ .

The data collected in this last measurement allow us to check the uniformity of the measured complexity across the 8 measurements for each basis setting. The NCD values corresponding to each trial are shown in figure 6. It is evident how the complexity of the generated strings do not vary significantly between trials, with a maximum variation of the order of 2%, supporting the uniform complexity assumption.

## 7. Discussion

There is a trend to look at physical systems and processes as programs run on a computer made of the constituents of our universe. Although this point of view has been already extensively used in quantum information theory, we present a complementary algorithmic approach for an explicit, experimentally testable example. This algorithmic approach is complementary to the orthodox Bell inequality approach to quantum

nonlocality [1] that is statistical in its nature.

The Kolmogorov complexity of the output of UTM must obey distance properties as shown in [8, 4], and can be approximated by compression. The distance properties lead to inequality (9), which we find violated in the specific case of polarization-entangled photon pairs. Therefore, no hidden variables can be encoded as programs for spatially separated UTMs, with the additional assumption of *uniform complexity* for our specific experimental implementation of the test.

We would like to stress that our analysis of the experimental data is purely and consistently algorithmic. This approach does not use the notion of an ensemble and the assumption that each bit in a data string comes from an i.i.d. source. The compression treats the string of data as a single entity, and does not ignore correlations between subsequent string elements.

We have become aware of a recent article by Wolf [24] where this algorithmic approach is used to provide a different viewpoint on nonlocality that does not require counterfactual reasoning.

## Acknowledgments

We acknowledge the support of this work by the National Research Foundation & Ministry of Education in Singapore, partly through the Academic Research Fund MOE2012-T3-1-009. P.K. and D.K. are also supported by the Foundational Questions Institute (FQXi). A.C. also thanks Andrea Baronchelli for the suggestions on the use of compression software.

- [1] Bell J S 1964 *Physics* **1** 195–200
- [2] Braunstein S L and Caves C M 1988 *Phys. Rev. Lett.* **61** 662–665 URL <http://link.aps.org/doi/10.1103/PhysRevLett.61.662>
- [3] Shannon C E 1948 *Bell System Technical Journal* **27** 379–423 URL <http://ieeexplore.ieee.org/lpdocs/epic03/wrapper.htm?arnumber=6773024>
- [4] Cilibrasi R and Vitányi P M B 2005 *Information Theory, IEEE Transactions on* **51** 1523–1545
- [5] Fuchs C A 1992 Algorithmic information theory and the hidden variable question *Workshop on Squeezed States and Uncertainty Relations* NASA Conference Publication 3135 ed Han D, Kim Y S and Zachary W W (NASA, Washington, DC) pp 83–85
- [6] Gill R D 2003 Time, finite statistics, and Bell’s fifth position *Proc. of “Foundations of Probability and Physics - 2” (Ser. Math. Modelling in Phys., Engin., and Cogn. Sc. vol 5 2002)* (Växjö Univ. Press) pp 179–206
- [7] Deutsch D 1985 *Proceedings of the Royal Society of London A: Mathematical, Physical and Engineering Sciences* **400** 97–117
- [8] Li M, Chen X, Li X, Ma B and Vitányi P M B 2004 *Information Theory, IEEE Transactions on* **50** 3250–3264
- [9] Santos E 1986 *Physics Letters A* **115** 363–365
- [10] Schumacher B W 1991 *Phys. Rev. A* **44** 7047–7052
- [11] Kurzyński P and Kaszlikowski D 2014 *Phys. Rev. A* **89** 012103
- [12] Wajs M, Kurzyński P and Kaszlikowski D 2015 *Phys. Rev. A* **91** 012114
- [13] Cover T M and Thomas J A 2006 *Elements of Information Theory* 2nd ed (Wiley-Interscience) ISBN 9780471748816
- [14] Pavlov I <http://www.7-zip.org/sdk.html> URL <http://www.7-zip.org/sdk.html>

- [15] Seward J <http://www.bzip.org/> URL <http://www.bzip.org>
- [16] Gailly J L and Adler M <http://www.gzip.org/> URL <http://www.gzip.org/>
- [17] Welch T 1984 *Computer* **17** 8–19 ISSN 0018-9162
- [18] MATLAB R2010a, The MathWorks, Inc., Natick, Massachusetts, United States.
- [19] Matsumoto M and Nishimura T 1998 *ACM Transactions on Modeling and Computer Simulation (TOMACS)* **8** 3–30
- [20] Marsaglia G and Tsang W W 2000 *Journal of Statistical Software* **5** 1–7 ISSN 1548-7660 URL <http://www.jstatsoft.org/v05/i08>
- [21] Kwiat P G, Mattle K, Weinfurter H, Zeilinger A, Sergienko A V and Shih Y 1995 *Phys. Rev. Lett.* **75** 4337–4341 URL <http://link.aps.org/doi/10.1103/PhysRevLett.75.4337>
- [22] Kurtsiefer C, Oberparleiter M and Weinfurter H 2001 *Phys. Rev. A* **64** 023802
- [23] Clauser J F, Horne M, Shimony A and Holt R 1969 *Phys. Rev. Lett.* **23** 880–884
- [24] Wolf S 2015 *Phys. Rev. A* **92**(5) 052102 URL <http://link.aps.org/doi/10.1103/PhysRevA.92.052102>